The Role of Flexure Margins in Controlling Open Fracture Distribution: Insights from Analogue Modeling of Orthogonal Rift and Pull-Apart Systems

Terry Alfa Furqan[1] and Benyamin Sapiie[1]

1. Institut Teknologi Bandung

Abstract

Hydrocarbon exploration in Basement Fracture Reservoirs faces significant challenges in predicting fracture connectivity below seismic resolution. This study utilizes analogue sandbox modeling to compare the spatial distribution of open fractures in orthogonal normal fault systems and pull-apart basins. Methodological innovation is implemented through the use of a 1 mm thick gypsum layer atop 8 cm of Ngrayong Formation sand, serving as a brittle rheological interface to simulate the mechanical response of the basement top. Experimental results demonstrate that open fractures are consistently localized within the flexure margin zone. In the orthogonal system, fractures exhibit a broad and elongated distribution parallel to the master fault, governed by the fault's total length. Conversely, the pull-apart system yields a narrower and more localized fracture network, predominantly concentrated within the inter-fault transfer zones at the master fault tips, with additional margin-parallel fractures and an intra-basin damage zone developing at high cumulative strains. The direct inter-fault connectivity observed in the pull-apart transfer zones is geometrically consistent with a higher proportion of X and Y-node configurations relative to the orthogonal system, suggesting superior fracture network connectivity in pull-apart settings. This study proposes an evolved paradigm in fracture prediction, suggesting that traditional distance-to-fault methods can be significantly enhanced by incorporating the estimation of cumulative extensional strain via streamlined 3D palinspastic restoration. The findings confirm that topographic curvature is only valid as a fracture indicator when genetically associated with active flexural bending mechanisms. For exploration practitioners, this study provides a direct, tectonic-regime-specific framework for delineating basement reservoir sweet spots and reducing dry-hole risk in fractured basement plays across Indonesia.

Introduction

Hydrocarbon exploration within Basement Fracture Reservoirs has become one of the primary focus areas in both global and domestic oil and gas industries, particularly in mature basins across Indonesia, such as the South and Central Sumatra Basins (Figure 1). Unlike conventional clastic reservoirs, the basement—typically composed of granitoid igneous or metamorphic rocks—exhibits negligible or non-existent matrix porosity. Consequently, the productivity of these reservoirs relies entirely on the presence of secondary porosity in the form of open fracture networks that function as both storage space and flow pathways (Nelson, 2001). Success in predicting fracture zones with high density and robust connectivity is a decisive factor in mitigating the high economic risk associated with dry holes in basement plays, ultimately determining the effectiveness of exploration drilling (Sapiie, 2005).

Despite the vital role of fractures, their architecture and quality are intrinsically governed by the local tectonic regimes that formed them. A fundamental, yet often underappreciated, limitation of conventional fracture prediction is the widespread use of 'distance-to-fault' analysis, which applies arbitrary buffer zones around mapped faults without accounting for the actual mechanical deformation field. This approach conflates proximity to a fault with the likelihood of open fracture occurrence, which may lead to significant mischaracterization of reservoir quality. Two commonly encountered

extensional systems with distinct reservoir characteristics are orthogonal normal fault systems and pull-apart basin systems. In pure extensional systems, tensile forces tend to generate fractures parallel to the strike of the master normal fault, following Andersonian shear failure principles (McClay, 1990). Conversely, in pull-apart systems involving a shear component (transtension), the interaction between master faults often creates more complex and overlapping fault segments, with structurally significant transfer zones developing between the fault tips to kinematically link the bounding master faults.

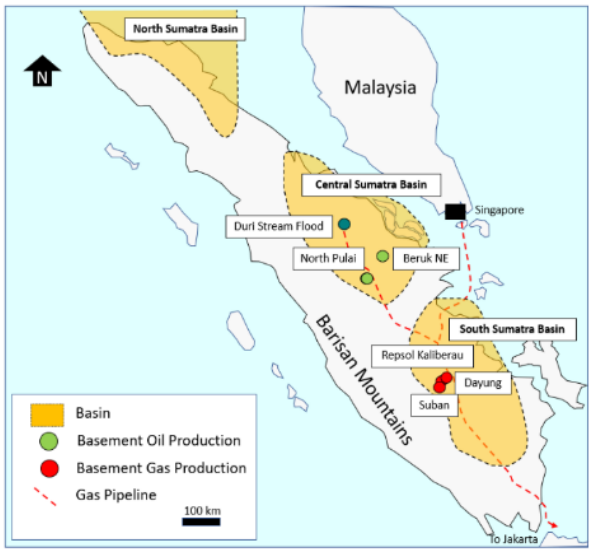

Figure 1. Location map of South and Central Sumatra Basins, highlighting known basement fracture reservoir fields (Koning et al., 2021)

A major challenge remains in differentiating connectivity quality and fracture aperture distribution between these two systems, especially when relying on seismic data with limited resolution at basement depths. To overcome the limitations of direct subsurface observation, physical analog sandbox modeling serves as a highly effective method for dynamically and mechanically visualizing structural evolution (Dooley & Schreurs, 2012). To systematically investigate fracture development within these evolving extensional fault systems, a thin layer of gypsum was applied to the surface of the models. This cohesive capping layer ensured structural integrity, effectively preventing the gravitational collapse of the granular material and preserving the geometry of the open fractures following their initiation.

This research aims to perform a comparative descriptive analysis of the open fracture characteristics formed in orthogonal normal fault versus pull-apart systems, with a primary focus on identifying fracture localization within the flexure margins of both systems. This comparative approach directly informs the central argument of this paper: open fractures developed within flexure margins exhibit significantly more extensive connectivity compared to the localized fracture networks governed merely by direct fault proximity. Utilizing a descriptive structural geology approach, this study provides insights into basement reservoir quality indicators applicable to hydrocarbon exploration strategies in complex tectonic settings. Furthermore, this research serves as a preliminary investigation to quantify fluid flow models based on surface fracture distributions. By employing the I-Y-X topological node classification method (Sanderson & Nixon, 2015), this work establishes a critical foundation to bridge empirical structural observations with future numerical modeling.

Methodology

Experimental Apparatus and Model Configuration

Analog sandbox modeling was implemented to simulate and compare the development of open fractures across two distinct tectonic regimes. Both models were constructed within a deformation box measuring 150 cm (length) × 50 cm (width) × 50 cm (depth). The experiments were conducted using a high-precision deformation box with the following kinematic setups:

- **Orthogonal Rift System (Model A; Figure 2):** This setup incorporated listric-shaped wooden blocks to replicate the basement master fault geometry. A flexible mylar sheet was placed between the blocks and the granular material to minimize basal friction, ensuring deformation was governed strictly by block geometry and the detachment plane. The experiment involved displacing the mylar sheet away from the basement blocks to induce pure extensional lengthening.
- **Oblique Pull-Apart System (Model B; Figure 3):** This configuration modeled a strike-slip step-over geometry using two wooden blocks. The primary variable was the distance of the step-over width, which was represented by the initial lateral gap between the basal blocks prior to deformation. Simultaneous divergence of the blocks induced subsidence in the overlying sand, generating normal faults characteristic of a pull-apart basin architecture.

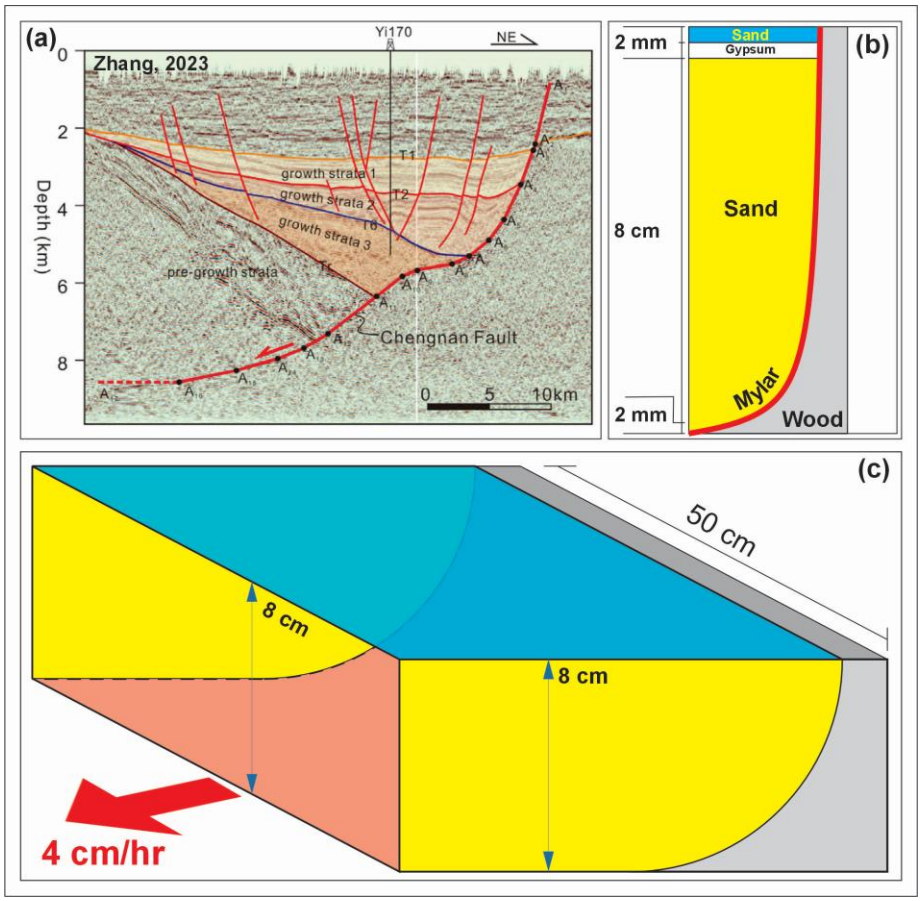

Figure 2. Experimental design and natural analog basis for the listric normal fault model. **(a)** Example of seismic reflection profile from the Bohai Bay Basin, Eastern China (Zhang, 2023), illustrating the characteristic rollover anticline and hanging-wall geometry associated with natural listric normal fault systems. **(b)** Schematic cross-

section of the experimental stratigraphic analog setting. The sand packet simulates the mechanical behavior of deformable upper crustal material, the flexible Mylar sheet simulates the basal detachment surface, and the rigid wooden block represents the undeformed crystalline footwall. **(c)** Three-dimensional block diagram of the pre-deformation experimental configuration. Progressive lateral extraction of the Mylar sheet (red surface; red arrow) induces gravitational collapse and translational displacement of the overlying sand mass, dynamically conforming the deforming wedge to the prescribed basement geometry and replicating the kinematic evolution of natural listric fault systems.

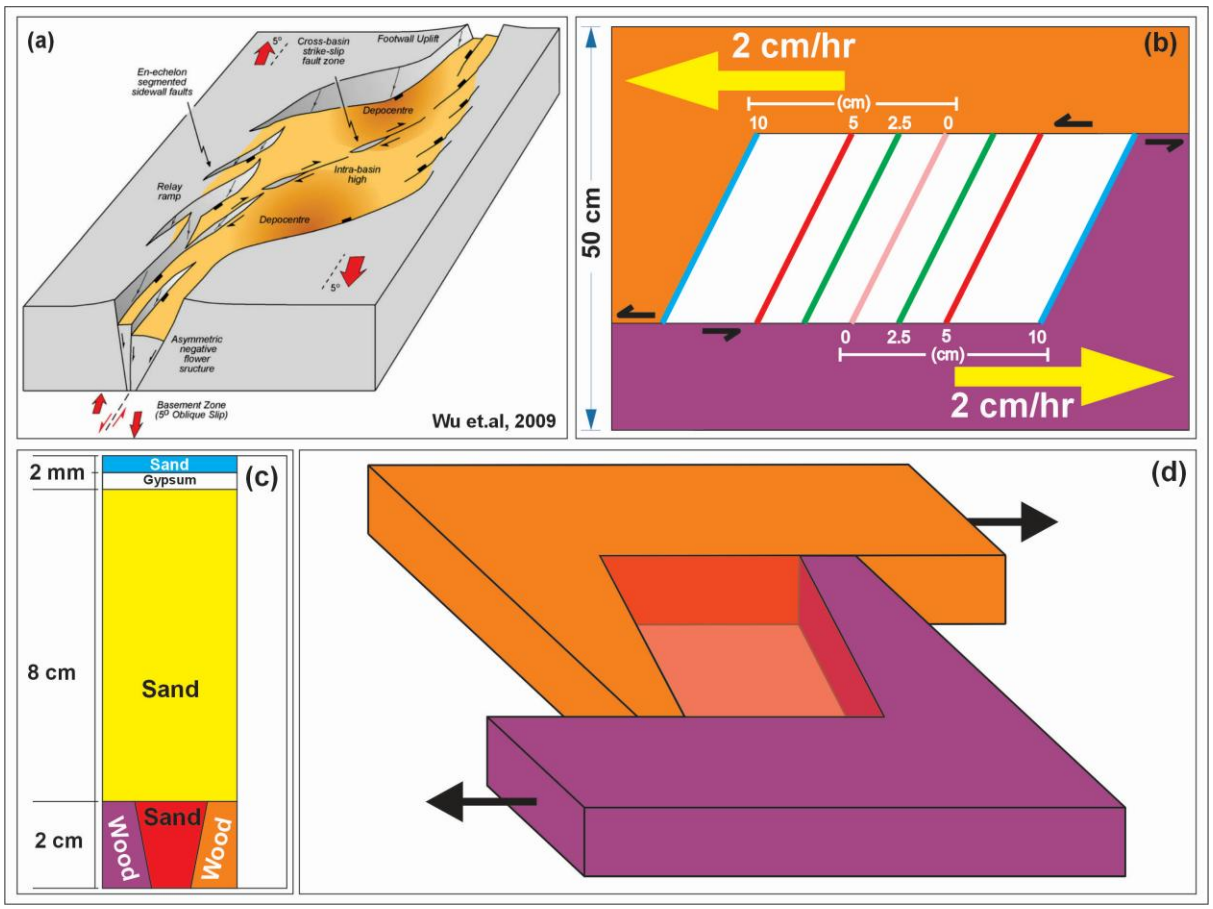

Figure 3. Conceptual framework and analog model design for pull-apart basin experiments. **(a)** Three-dimensional schematic of an idealized natural pull-apart basin (modified from Wu et al., 2009). **(b)** Map-view of kinematic diagram of the experimental configuration. Antipodal displacement of the rigid basement blocks at equal velocities (2 cm/hr each) generates a cumulative sinistral strike-slip rate of 4 cm/hr across the releasing stepover zone; initial gap widths (colored intervals) were systematically varied to assess the influence of stepover distance on basin geometry and fault architecture. **(c)** Cross-sectional stratigraphy of the experimental setup. Rigid wooden blocks represent the undeformed crystalline basement, the overlying sand pack simulates the shallow deformable crystalline basement rock mass, and the basal red sand layer demarcates the highly strained inter-fault accommodation zone. **(d)** Three-dimensional basal block geometry. The central rectangular void, initially infilled with red-dyed sand, provides vertical accommodation space to facilitate progressive basin floor subsidence during transtensional deformation.

Both models were driven at a constant rate with a total extension speed of 4 cm per hour. Given that the granular analogue materials employed in this study lack time-dependent mechanical properties such as viscosity, the deformation rate does not enter into the geometric scaling relationships established by Hubbert (1937). Accordingly, the displacement velocity was selected to be as low as practically feasible, approximating quasi-static deformation conditions in which structural evolution is governed exclusively by block geometry and basal friction, rather than by inertial or rate-dependent effects. This approach ensures that time-lapse observations accurately reflect the kinematic sequence of fracture initiation and propagation (Furqan et al., 2024).

Materials and Model Stratigraphy

The experimental design focused on simulating the mechanical response of a competent crystalline basement. To accurately capture both bulk deformation and high-resolution fracture geometries, the model stratigraphy was constructed using three distinct functional layers:

1. Basement Analog Layer: An 8 cm thick sequence of natural, cohesionless Ngrayong Formation sand. Possessing a well-characterized internal friction angle, this layer serves as the primary mechanical analog for crystalline basement rock deforming within a brittle regime.
2. Cohesive Capping Layer: A 1 mm thick application of pure gypsum powder. This layer simulates a brittle surface condition highly susceptible to fracturing. Crucially, the cohesive nature of the gypsum preserves the morphology of the open fractures by preventing the immediate gravitational collapse that typically obliterates fracture void spaces in purely cohesionless sand. Given its negligible thickness, this layer ensures structural preservation without altering the fundamental mechanical scaling factors of the bulk model.
3. Visual Contrast Layer: A final 1 mm thick veneer of blue-dyed sand applied over the gypsum. Because the highly reflective, white surface of the underlying gypsum causes undesirable glare under experimental illumination, this uppermost sand layer mitigates light reflection and significantly enhances the macroscopic photographic contrast of the developing fracture apertures.

Data Acquisition and Descriptive Observation

The evolution of open fractures was recorded using a high-resolution digital camera mounted in a nadiral (top-view) position. Time-lapse photography monitored structural development from initiation to the final stage, with 30 sec interval. Primary analysis involved qualitative visual observation of the surface photographs to identify fracture localization, assess the consistency of structural evolution, and determine the dominant spatial distribution patterns.

Qualitative visual observation of the final-stage photographs was conducted to characterize fracture connectivity differences between the two tectonic systems. In the pull-apart basin experiments, direct inter-fault connectivity between opposing master faults was observed within the transfer zones; following the geometric framework of Sanderson & Nixon (2015), such connectivity patterns are geometrically consistent with the presence of X and Y-node configurations — where fracture segments intersect or terminate against one another — as opposed to the isolated I-node-dominated arrays expected in systems lacking inter-fault linkage.

Results and Discussion

Analog Sandbox Modeling Results

Based on the analog sandbox modeling experimental results for both systems, it was observed that open fractures consistently formed and extensively connected within the Flexure Margin of the resulting basins. Although both models exhibited fracture development within the gypsum, the spatial distribution and localization of these fractures showed significant differences depending on the tectonic regime:

1. Orthogonal System (Figure 4): Open fractures consistently localized within the flexure margin at the monocline crest, oriented parallel to the master normal fault. This spatial restriction demonstrates that fault geometry—rather than mere proximity—is the primary mechanical control on fracture distribution, with direct implications for regional sweet-spot delineation.
2. Pull-Apart Basin System (Figures 5 and 6): The flexure margin localized at the tips of the paired master normal faults, manifesting as high-intensity fracturing within the inter-fault transfer zones. Fracture patterns exhibited markedly higher geometric complexity than the orthogonal system; most notably, direct inter-fault connectivity between opposing master faults was observed within the transfer zones across all step-over configurations. Following the geometric framework of Sanderson & Nixon (2015), such inter-fault linkage is geometrically consistent with a higher proportion of X and Y-node configurations relative to the isolated, I-node-dominated arrays of the orthogonal system — an inference that carries significant implications for hydraulic connectivity in subsurface analogs. The systematic variation in basin architecture as a function of step-over width is comprehensively documented in Figure 6.

Table 1 below summarizes the key qualitative geometric differences observed between the two models:

Table 1. Qualitative comparison of fracture characteristics between Model A (Orthogonal) and Model B (Pull-Apart).

Parameter	Model A (Orthogonal)	Model B (Pull-Apart)
Fracture orientation	Mostly parallel to master fault	Oblique; X and Y-node dominated
Fracture zone extent	Controlled by master fault length	Controlled by step-over width
Fracture density (qualitative)	Moderate; uniform	Higher; more complex intersections
Dominant node type	I and Y nodes	X and Y nodes
Reservoir 'sweet spot' predictor	Master fault length	Step-over zone dimensions

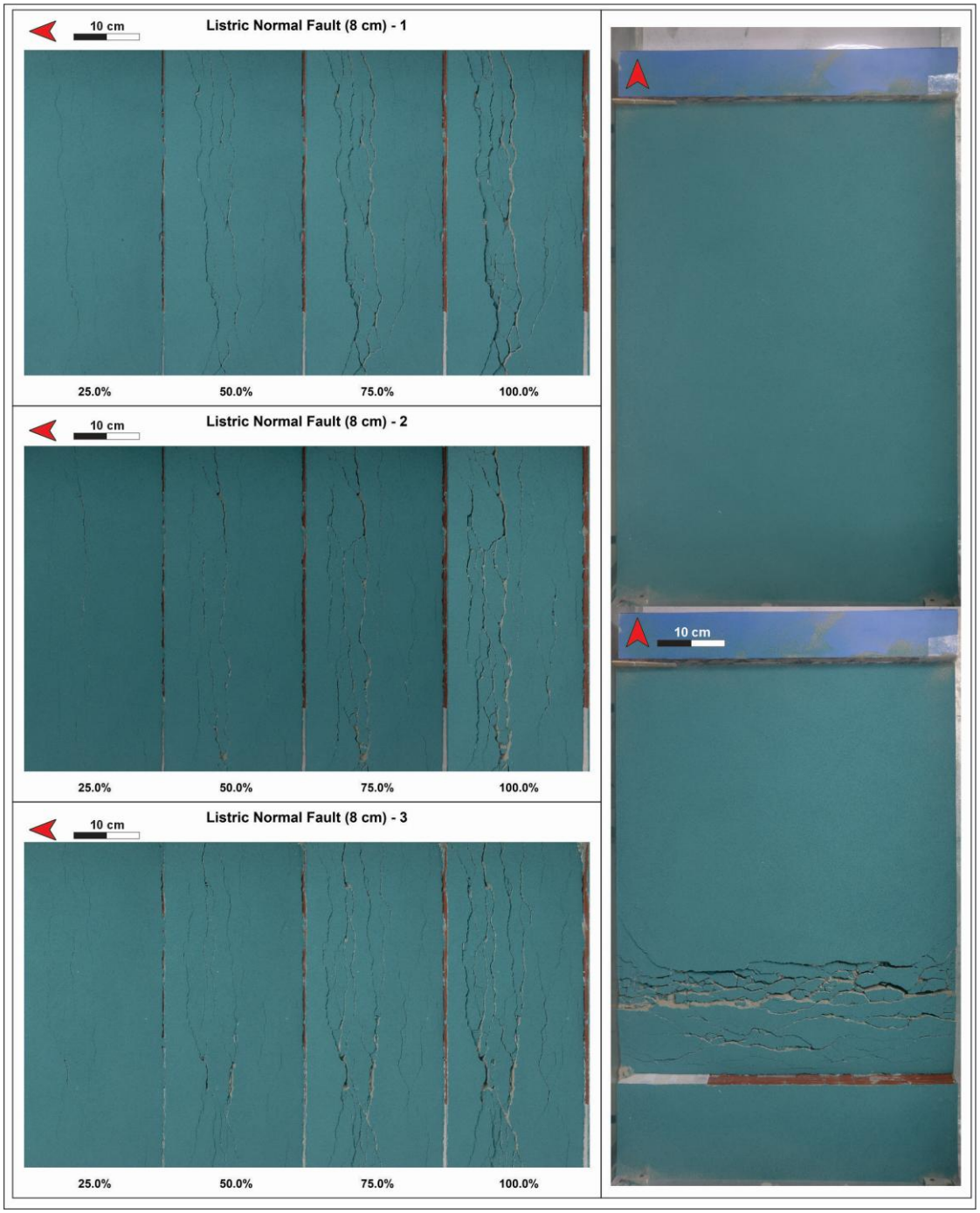

Figure 4. Map-view photographic sequence documenting the progressive structural evolution of listric normal fault analog experiments (initial sand pack thickness: 8 cm). Red arrows denote the kinematic transport direction of the basal detachment. The left column presents cropped plan-view images of the deformation zone across three independent experimental iterations (Runs 1–3), illustrating the sequential development of extensional fractures at 25%, 50%, 75%, and 100% of total applied extension (maximum heave: 2 cm). The right column contrasts the initial undeformed configuration (top) with the final structural assemblage (bottom). Macroscopically, open fractures are systematically localized within the zone of maximum structural curvature, consistently defining a well-developed flexural margin. These observations support the hypothesis for further research that initial overburden thickness — as a proxy for depth

to detachment — and master fault geometry exert first-order controls on fracture distribution patterns.

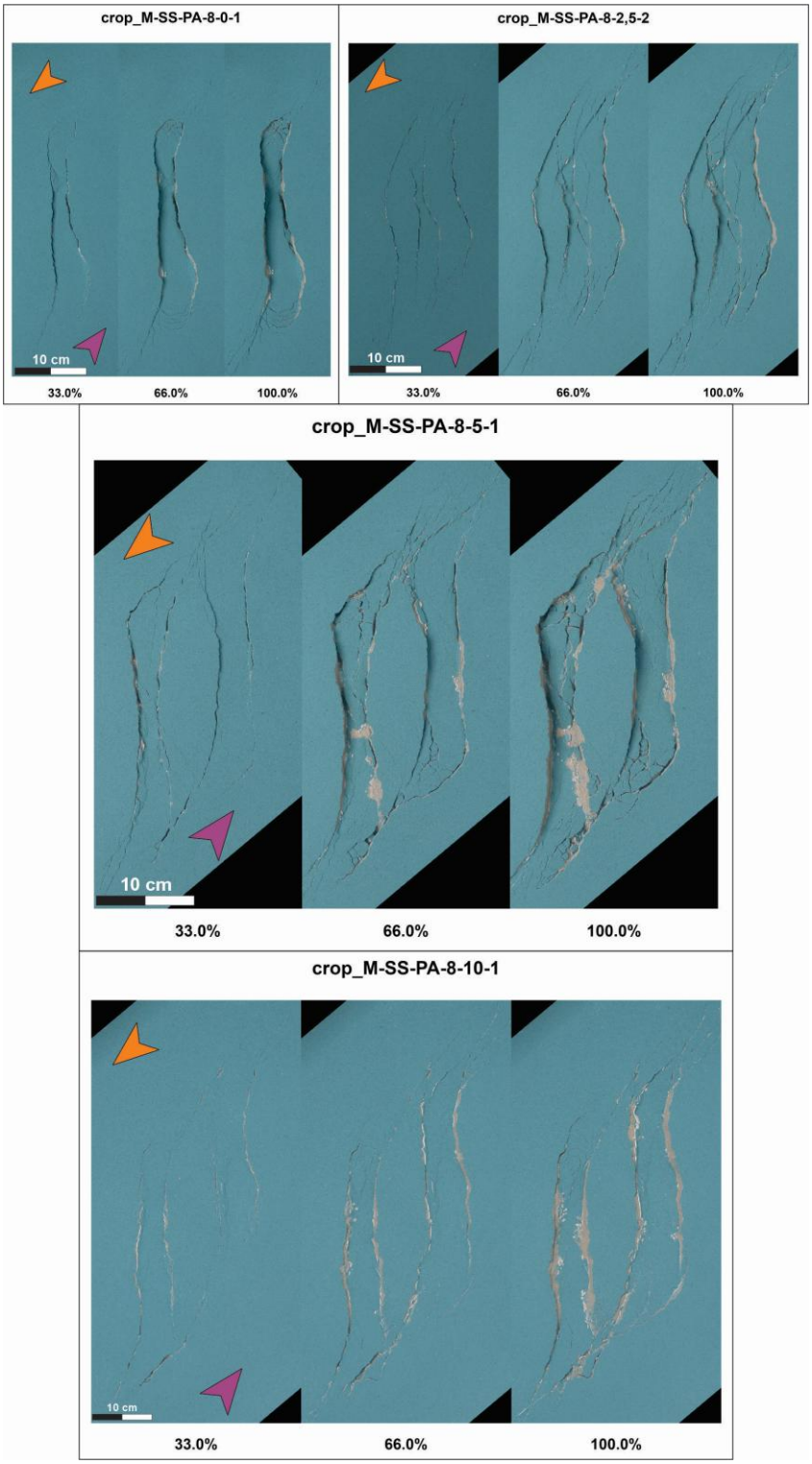

Figure 5. Map-view kinematic evolution of the pull-apart basin models across varying initial step-over widths (0, 2.5, 5, and 10 cm). The photographic sequence illustrates progressive structural development at 33%, 66%, and 100% of the total lateral displacement (2 cm). Orange and purple arrows denote the applied sinistral shear couple. At early strain intervals (33%), deformation is exclusively accommodated by the initiation of basin-bounding master normal faults; open fractures associated with

flexural-margin are notably absent. The emergence of these intra-basin open fractures—which potentially serve as critical kinematic linkages between the bounding master faults—is restricted to higher strain accumulations (≥66%). This temporal delay indicates that flexure-induced fracturing requires a specific threshold of basin subsidence and structural deepening prior to initiation.

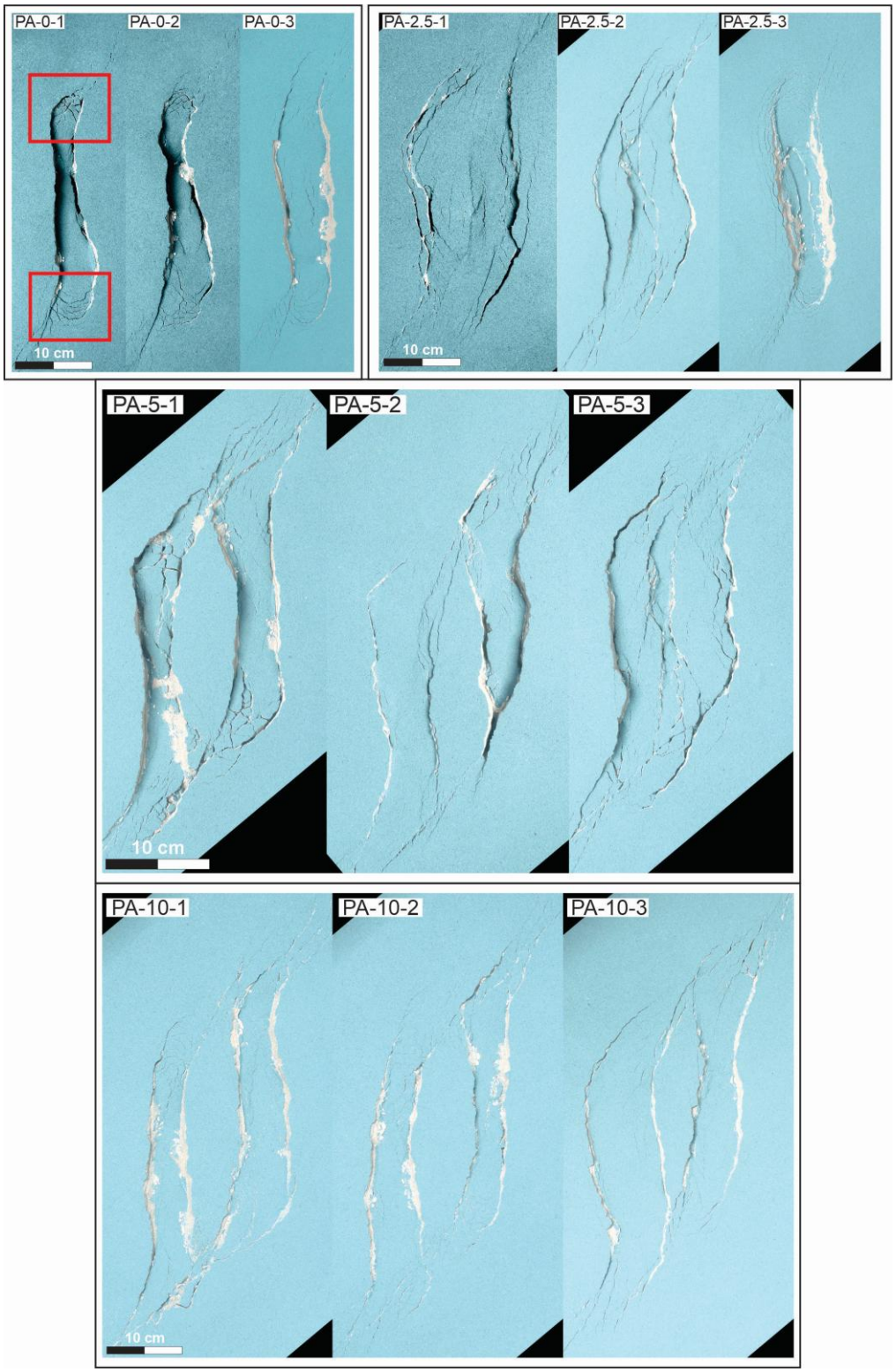

Figure 6. Final map-view structural configuration of the pull-apart basin models at maximum lateral displacement (100% strain; 2 cm). The collage presents three

independent iterations for each initial step-over width (0, 2.5, 5, and 10 cm) to demonstrate macro-scale reproducibility. Red boxes highlight the "transfer zones", which act as critical kinematic linkages dominated by high-intensity open fractures connecting the opposing master faults. In the 0 cm step-over case, the deformation is geometrically analogous the orthogonal listric normal faulting, generating a central depocenter flanked by distinct rollover anticlines. In the 2.5 cm step-over configuration, alongside the persistent formation of open fractures within the transfer zones, additional fractures emerge parallel to the basin-bounding master faults at high cumulative strains. These margin-parallel features are kinematically associated with a developing cross-basin strike-slip fault zone; progressive strain partitioning localizes significant shear within the basin center, fostering a highly fractured intra-basin damage zone. Conversely, wider step-overs (5 cm and 10 cm) produce structural compartmentalization through the formation of a central intra-basin high (horst). Despite this compartmentalization, high-intensity fracturing within the transfer zones (red boxes) remains consistent across all configurations. Furthermore, qualitative observation reveals that the vertical displacement (throw) of the master faults decreases from the 5 cm to the 10 cm configuration. This attenuation reflects the broader spatial distribution of extensional strain induced by the wider basal gap.

Geometric Control on Fracture Quality

Observations from both models indicate that the extent and distribution of the flexure margin — a key indicator of basement reservoir quality — are governed by fundamentally different geometric parameters in each tectonic regime.

The Orthogonal System: The areal extent of the flexure margin is primarily determined by the length of the master normal fault (Figure 4). The longer the master fault, the more extensive the monocline at the fault crest that accommodates open fracture formation, suggesting that basement reservoir sweet spots in pure rifting systems are likely to follow regional major fault trends.

The Pull-Apart System: The fracture zone area is primarily governed by the width of the step-over zone — the distance between the bounding master faults (Figure 6). The accommodation space generated by lateral shear produces localized stress concentrations that drive the development of geometrically complex open fractures between the two master faults. Critically, the inter-fault connectivity observed within the transfer zones of this system is geometrically consistent with a higher prevalence of X and Y-node configurations — as defined by Sanderson & Nixon (2015) — relative to the orthogonal system. This inference implies that, despite the more restricted areal extent of the fracture zone, pull-apart fracture networks may exhibit superior hydraulic connectivity relative to the broader but structurally simpler arrays characteristic of orthogonal systems.

A New Paradigm for Subsurface Fracture Prediction

These modeling results offer a fresh perspective on fracture prediction methods, which have traditionally relied heavily on "distance-to-fault" analysis. This conventional approach imposes hypothetical buffer zones around mapped faults that bear no direct mechanical relationship to the actual deformation field. Applying the geometric scaling relationship of Hubbert (1937), the $1{:}10^{-5}$ length ratio of the sandbox model implies that the master faults observed in the experiments correspond to structures on the order of kilometers in nature. Conventional distance-to-fault buffer zones applied in exploration practice typically span hundreds of meters — a distance that, when scaled to model dimensions, corresponds to only a few millimeters from the master fault trace. Critically,

visual inspection of the experimental surface immediately adjacent to the master faults reveals no significant open fracture development within this scaled equivalent zone; fractures are instead systematically restricted to the flexure margin, located at a structurally meaningful distance from the master fault. Our observations therefore demonstrate that open fracture distribution at the flexure margin — a localized zone of high tensile strain — is more mechanically meaningful and spatially predictable than what is implied by arbitrary distance parameters.

In data-poor subsurface environments, fracture distribution at the flexure margin can be estimated through a streamlined 3D palinspastic restoration approach. The fundamental premise of this approach is that the present-day geometry of a subsurface horizon preserves a record of the cumulative strain imposed by the faults that shaped it. By restoring a single key horizon — most practically, the top-basement surface — to its inferred initial horizontal configuration, one can reconstruct the strain history experienced by that surface and identify zones of anomalously high extensional strain. This restoration assumes that the surface was originally planar and horizontal prior to deformation, a working assumption that must be evaluated against available stratigraphic and seismic data in any given study area. The analogue models presented here demonstrate that this extensional strain is geometrically predictable from the structural configuration (fault length for orthogonal systems; step-over width for pull-apart systems), providing a viable first-order basis for estimating fracture occurrence probability and sub-seismic connectivity in a given zone.

These findings also carry implications for the use of topographic curvature analysis in fracture prediction. Only curvature genetically associated with active flexural bending mechanisms mechanically contributes to open fracture generation through outer-arc extension; curvature resulting from passive draping or differential compaction may not involve sufficient tectonic force to open fractures, potentially generating false positives in reservoir quality interpretation. It should be noted, however, that this distinction constitutes an inference based on mechanical principles rather than a result directly tested in this experimental campaign — the sandbox experiments presented here exclusively simulate active flexural bending. Future studies incorporating velocity-stratified models could explicitly test this contrast.

Conclusion

Based on the comparative descriptive study through analog sandbox modeling, several key conclusions are drawn:

1. Open fractures in both tectonic regimes consistently localized within the flexure margin. In the orthogonal normal fault system, this zone is located at the monocline crest parallel to the master fault, whereas in the pull-apart system, it is concentrated within the inter-fault transfer zones — with fracture complexity and spatial distribution varying systematically as a function of step-over width.
2. The areal extent of the flexure margin is governed by different geometric parameters in each regime: the length of the master normal fault in orthogonal systems, and the dimensions of the step-over zone in pull-apart systems.
3. Fracture distribution at the flexure margin is interpreted to be more mechanically meaningful and spatially predictable through the estimation of cumulative extensional strain from streamlined 3D palinspastic restoration than through conventional distance-to-fault methods. Curvature analysis remains a viable tool, but must be applied cautiously and is only interpretable as a fracture indicator where active flexural bending can be independently confirmed.

4. The direct inter-fault connectivity observed within the pull-apart transfer zones implies that pull-apart fracture networks, despite their more restricted areal extent, are geometrically consistent with a higher prevalence of X and Y-node configurations than the orthogonal system — indicating superior intrinsic connectivity with significant implications for productivity prediction in basement reservoir plays. This connectivity inference constitutes a foundational preliminary step toward a tectonic-regime-specific Discrete Fracture Network (DFN) fluid flow model, and its formal quantification is identified as the immediate next phase of this research program.

Acknowledgements

The author would like to thank Institut Teknologi Bandung (ITB) for funding this research through the National Post-Doctoral Equity Research Program (Program Equity Post-Doctoral Dalam Negeri). Gratitude is also extended to the Geodynamics and Sedimentology Research Group, ITB, for providing access to the sandbox laboratory facilities. Special thanks to Didin Saepudin for his consistent and invaluable technical assistance as a laboratory technician throughout the experimental process. The authors also wish to express their sincere gratitude to Mr. Reksalegora for his thorough and constructive review, which provided invaluable critical insights that significantly contributed to the refinement and improvement of this manuscript.

References

Dooley, T. P., & Schreurs, G. (2012). Analogue modelling of intraplate strike-slip tectonics: A review and new experimental results. *Tectonophysics*, *574–575*, 1–71. https://doi.org/10.1016/j.tecto.2012.05.030

Furqan, T. A., Sapiie, B., Natawidjaja, D. H., Widodo, L. E., Rudyawan, A., & Hadiana, M. (2024). Fault Surface Rupture Modeling Using Particle Image Velocimetry Analysis of Analog Sandbox Model. *Journal of Engineering and Technological Sciences*, *56*(1), 125–141. https://doi.org/10.5614/j.eng.technol.sci.2024.56.1.10

Hubbert, M. K. (1937). Theory of scale models as applied to the study of geologic structures. *Bulletin of the Geological Society of America*, *48(10)*.

Koning, T., Cameron, N., & Clure, J. (2021). Undiscovered Potential in the Basement Exploring in Sumatra for oil and gas in naturally fractured and weathered basement reservoirs. *Berita Sedimentologi*, *47*(2), 67–79. https://doi.org/10.51835/bsed.2021.47.2.320

McClay, K. R. (1990). Extensional fault systems in sedimentary basins: A review of analogue model studies. *Marine and Petroleum Geology*, *7*(3), 206–233. https://doi.org/10.1016/0264-8172(90)90001-W

Sanderson, D. J., & Nixon, C. W. (2015). The use of topology in fracture network characterization. *Journal of Structural Geology*, *72*, 55–66. https://doi.org/10.1016/j.jsg.2015.01.005

Sapiie, B. (2005, January 1). Analogue modeling of rift mechanism in the paleogene graben system of Western Indonesia. *Proc. Indon Petrol. Assoc., 30th Ann. Conv.* Thirtieth Annual Convention. https://doi.org/10.29118/IPA.1373.05.G.186

Wu, J. E., McClay, K., Whitehouse, P., & Dooley, T. (2009). 4D analogue modelling of transtensional pull-apart basins. *Marine and Petroleum Geology*, *26*(8), 1608–1623. https://doi.org/10.1016/j.marpetgeo.2008.06.007

Zhang, Y. (2023). A geometric analysis of slip rate variation with depth in listric normal faults. *Frontiers in Earth Science*, *11*, 1266454. https://doi.org/10.3389/feart.2023.1266454